

Lab on a Chip

Accepted Manuscript



This is an *Accepted Manuscript*, which has been through the Royal Society of Chemistry peer review process and has been accepted for publication.

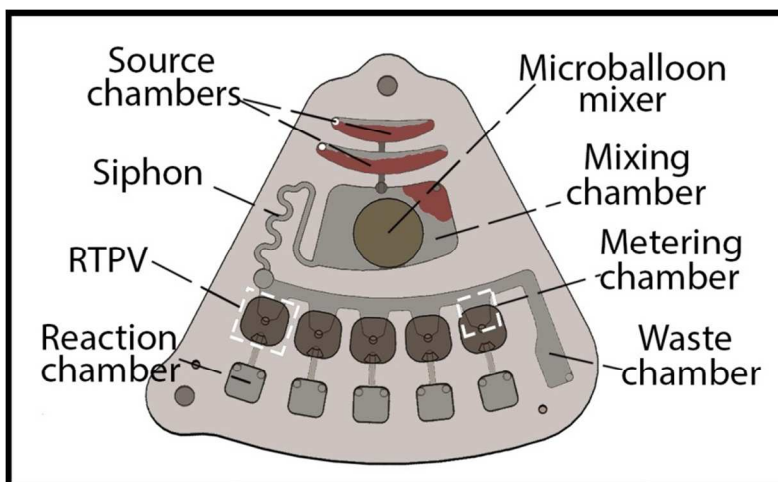
Accepted Manuscripts are published online shortly after acceptance, before technical editing, formatting and proof reading. Using this free service, authors can make their results available to the community, in citable form, before we publish the edited article. We will replace this *Accepted Manuscript* with the edited and formatted *Advance Article* as soon as it is available.

You can find more information about *Accepted Manuscripts* in the [Information for Authors](#).

Please note that technical editing may introduce minor changes to the text and/or graphics, which may alter content. The journal's standard [Terms & Conditions](#) and the [Ethical guidelines](#) still apply. In no event shall the Royal Society of Chemistry be held responsible for any errors or omissions in this *Accepted Manuscript* or any consequences arising from the use of any information it contains.

Reversible Thermo-Pneumatic Valves on Centrifugal Microfluidic Platforms

Reversible thermo-pneumatic valving (RTPV) technique is based on the deflection of an elastic latex membrane. Unlike conventional, single-use active valves that utilize thermal energy to remove barriers to permit liquid flow, RTPV is a reversible mechanism that manipulates thermal energy to reversibly block or open microchannels. We have experimentally and theoretically studied the operational mechanism of the RTPV over a range of rotational frequencies from 700 RPM to 2500 RPM and temperatures from 26 to ~70 °C. The ability of the valve to automatically close at elevated temperature prevented the evaporation of reagents during thermocycling periods. Hence, the RTPVs and microballoon pump/mixer are integrated in a microfluidic cartridge to automate a fluidic procedure required for multiplexing of temperature-controlled assays. As a pilot study, the cartridge is used for sequential aliquoting to prepare multiple separated PCR reaction mixtures for the detection of Dengue virus.



Reversible Thermo-Pneumatic Valves on Centrifugal Microfluidic Platforms

Cite this: DOI: 10.1039/x0xx00000x

Mohammad Mahdi Aeinehvand,^a Fatimah Ibrahim,^{*a} Sulaiman Wadi Harun,^{ab} Amin Kazemzadeh,^{ab} Hussin A. Rothan,^c Rohana Yusof,^c and Marc Madou^{ade}

Received 00th January 2012,
Accepted 00th January 2012

DOI: 10.1039/x0xx00000x

www.rsc.org/

Centrifugal microfluidic systems utilize a conventional spindle motor to automate parallel biochemical assays on a single microfluidic disk. The integration of complex, sequential microfluidic procedures on these platforms relies on robust valving techniques that allow for the precise control and manipulation of fluid flow. The ability of valves to consistently return to their former condition after each actuation plays a significant role in the real-time manipulation of fluidic operations. In this paper, we introduce an active valving technique that operates based on the deflection of a latex film with the potential for real-time flow manipulation in a wide range of operational spinning speeds. The reversible thermo-pneumatic valve (RTPV) seals or reopens an inlet when a trapped air volume is heated or cooled, respectively. The RTPV is a gas-impermeable valve composed of an air chamber enclosed by a latex membrane and a specially designed liquid transition chamber that enables the efficient usage of the applied thermal energy. Inputting thermo-pneumatic (TP) energy into the air chamber deflects the membrane into the liquid transition chamber against an inlet, sealing it and thus, preventing fluid flow. From this point, a centrifugal pressure higher than the induced TP pressure in the air chamber reopens the fluid pathway. The behaviour of this newly introduced reversible valving system on a microfluidic disk is studied experimentally and theoretically over a range of rotational frequencies from 700 RPM to 2500 RPM. Furthermore, adding a physical component (e.g., a hemispherical rubber element) to induce initial flow resistance shifts the operational range of rotational frequencies of the RTPV to more than 6000 RPM. An analytical solution for the cooling of a heated RTPV on a spinning disk is also presented, which highlights the need for the future development of time-programmable RTPVs. Moreover, the reversibility and gas-impermeability of the RTPV in the microfluidic networks are validated on a microfluidic disk designed for performing liquid circulation. Finally, an array of RTPVs is integrated on a microfluidic cartridge to enable sequential aliquoting for the conversion of Dengue virus RNA to cDNA and the preparation of PCR reaction mixture.

1. Introduction

'Lab-on-a-Chip' (LOC) devices utilize microfluidic elements such as pumps, mixers, and valves to miniaturize large laboratory machine functions onto small silicon or plastic substrates.¹ A subcategory of LOC devices is the microfluidic disk, also known as Lab on a Disc (LOAD), which utilizes pseudo forces during spinning to manipulate liquid flow within the microfluidic networks. The generated centrifugal force enables automatic parallel processing of intricate tasks on a single platform with no need for external pressure generating pumps.²⁻⁶ The arrangement of various microfluidic elements on a disk is usually designed with respect to the sequence of

fluidic steps in an analytical assay. The assay on the disk is then controlled through different valving techniques and spin profiles.^{7, 8} Some of the challenges regarding valving on microfluidic disks are limited operational range of rotational frequencies, lack of versatility, and low reliability.⁹⁻¹¹

The performance of centrifugal microfluidic systems strongly depends on the ability of the passive and active valving technique present to control liquid retention and flow. Passive valves prevent flow based on surface tension or a physical gating mechanism and can be actuated using a variation in the spinning speed.¹²⁻¹⁷ As an example, Centrifugo-pneumatic (CP) valves utilize trapped air to prevent liquid from flowing into ventless chambers.^{13, 18} This valve can be tuned to operate over

a large range of desired spinning frequencies but can be implemented only at the end of a fluidic path. To enable the use of CP valves for a wide range of applications, Gorkin *et al.* utilized a dissolvable film (DF) as the secondary flow barrier to form similar trapped air pockets at any desirable point in the fluidic pathway.^{9, 19-21} The CP valve and the DF valve are single-use valves and are unable to stop further liquid flow after the valve has been opened. Hwang *et al.* developed the elastomeric valve, a reversible passive valve whose closure depends on weak adhesive forces between polydimethylsiloxane (PDMS) and polycarbonate.²² Elastomeric valves can retain higher volumes of liquid only at low centrifugal pressure. Because it is a physical barrier that must be continuously opened by liquid pressure in order for the liquid to pass, the valve may not open if a small volume of liquid does not provide sufficient hydrostatic pressure.

Unlike passive valves, active valves can be opened or closed by external power sources.²³⁻²⁸ For instance, laser irradiated ferrowax microvalves and optofluidic valves are opened by focusing a heat or laser source on the sacrificial valves.^{29, 30} Valves that use sacrificial barriers granted more robust and precise control of flow on disk. However, valving technologies that are reversible, (i.e., able to switch between open and closed states), make a more sophisticated and flexible flow control system.

To this end, Cai *et al.* recently developed a magnetically actuated valve with an operating range of rotational frequencies from 800 to 1600 RPM.³¹ The magnetically actuated valve was composed of a PDMS membrane with a ball spacer on top of it, a pair of magnets (one located at the bottom of the disk and one on the top of the ball spacer), and a flyball governor for mechanically adjusting the distance between the magnets.³¹ At low rotational frequencies, the attraction force between two magnets deflected the membrane into the chamber and completely blocked a fluidic pathway. At higher speeds, the centrifugal force overcame the weight of the flyballs, increasing the distance between the magnets and opening the fluidic path. The distance-dependent interactions between multiple magnet pairs and their physical size limited the number of this valve that can be embedded in a disk. Moreover, the bulky and mechanically complex actuation system used in this technique prevents the integration of other hardware components potentially needed for other on-disk processes. Therefore, complex centrifugal microfluidic processes still demand the development of simpler, reversible valving systems that enable flexible and real-time control of flow.

Previously, our team implemented latex microballoon technology, which can be used for the passive valving, pumping, and mixing of liquid samples on microfluidic disks without the need for surface modification, high spinning speeds, or high disk acceleration rates.^{32, 33} In the current study, we demonstrate an additional utility of latex films by incorporating them into reversible, gas/liquid-impermeable microvalves designed for precise on-disk control of liquid and thermo-pneumatic (TP) energy flow. To this end, we introduce a real-time valving mechanism that we named the reversible thermo-pneumatic valve (RTPV) based on the thermal expansion or contraction of air trapped in the system and the deflection of a latex elastic membrane (i.e., microballoon). In this newly introduced valving mechanism, microfluidic pathways are closed by applying heat and reopened using a centrifugal pressure higher than the produced TP pressure.

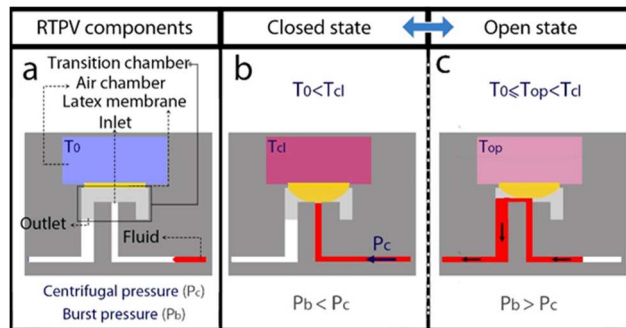


Figure 1. Schematic illustration of the mechanism of the reversible thermo-pneumatic valve (RTPV). (a) The RTPV components. (b) Closed state at a higher temperature. (c) Open state at room temperature i.e., the valve prevents fluid flow unless a centrifugal pressure higher than the TP pressure pushes back the membrane.

As a normally-open valve that requires heat to be closed, the RTPV is therefore a suitable valving solution in temperature-controlled assays such as polymerase chain reaction (PCR) and loop-mediated isothermal amplification (LAMP) assays. Here, the RTPV mechanism is investigated experimentally and theoretically in a range of rotational frequencies up to 2500 RPM. We have also analysed the cooling process of heated spinning disks to enable precise timing of the RTPV's actuation with various cooling spinning speeds. Moreover, an application of the RTPVs for continuous flow circulation was demonstrated to verify gas-impermeability and reversibility of the valve as well as its ability to control liquid and gas flow in complex microfluidic structures. Finally, RTPVs and microballoon pump/mixer are integrated in a microfluidic cartridge to automate a fluidic procedure required for multiplexing of temperature-controlled assays. As a pilot study, the cartridge is used for sequential aliquoting to prepare multiple separated PCR reaction mixtures for the detection of Dengue virus.

2. Materials and methods

2.1. Concept

PDMS and latex are popular materials for the fabrication of pneumatically and thermo-pneumatically (TP) actuated reversible microvalves in LOC microfluidic devices.³⁴⁻³⁸ On-off valves, push-up, and push-down valves developed by the Quake group, and latex membrane microvalves developed by the Mathies group constitute some examples of such sophisticated, practical PDMS- and latex-based valves.³⁸⁻⁴¹ Reversible valves have been used in various microfluidic applications, particularly for sample preparation and for the prevention of reagent evaporation at elevated temperatures.^{35, 41-43} In this study, we are developing a similar valving technology to TP actuated membranes on centrifugal microfluidic platforms.

The mechanism of the newly introduced valving system is based on the deflection of an elastic membrane (latex membrane) that can reliably close and reopen a fluid inlet perpendicular to the membrane. The valve, shown in Figure 1.a, consisted of a U-shaped transition chamber (i.e., composed of an inlet and an outlet for liquid flow), a latex membrane, and a ventless air chamber adjacent to the latex membrane to receive thermal energy. The membrane deflects when the ventless air chamber receives thermal energy and reverts back as the air chamber cools down to room temperature. Hence, the physical

components capable of this phenomenon are collectively named the RTPV. The membrane deflects into the transition chamber and pushes against the entrance of the perpendicular microchannel (inlet) to prevent fluid flow when the air chamber is heated (see Figure 1.b). For the valve to open during spinning, the hydrostatic pressure must overcome the induced TP pressure. An optimal spinning speed can generate sufficient centrifugal force to achieve the required hydrostatic pressure while performing passive cooling (see Figure 1.c).

2.2. Microfluidic disks design and fabrication

Three microfluidic platforms were created: Design A for the theoretical and experimental evaluation of the RTPV mechanism, and other designs (Design B and Design C) for demonstrating different applications of RTPVs on microfluidic

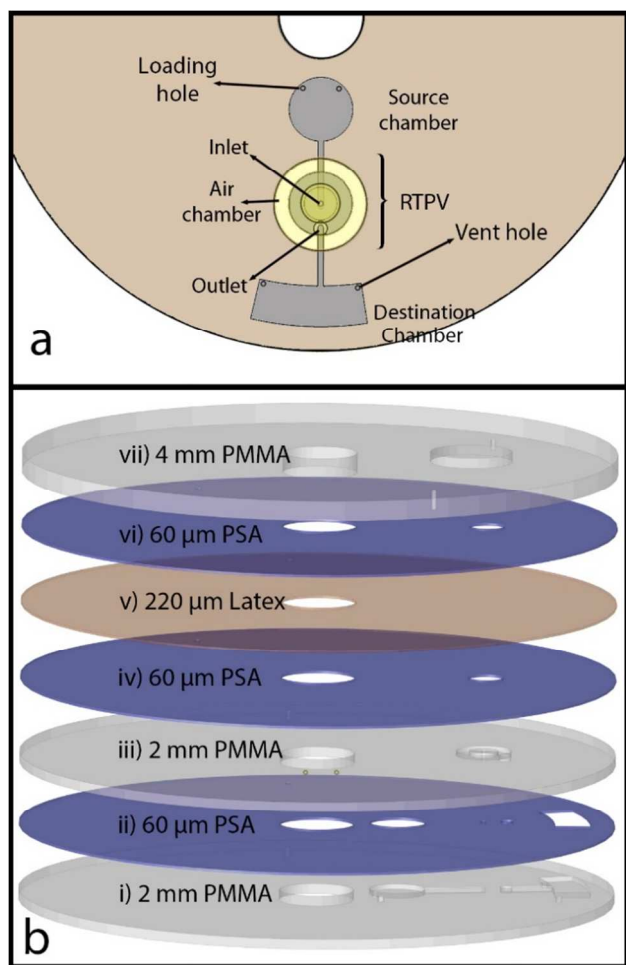


Figure 2. Microfluidic disk Design A. (a) Design A consists of a source chamber, an RTPV and a destination chamber. (b) The components of this microfluidic disk include three PMMA disks, three PSA layers, and a latex film. Layer i: the PMMA disk contains the loading/vent holes, engraved microchannels, source chamber, and destination chamber. Layer ii: An adhesive film with cut-outs in the shape of the source/destination chambers and through-holes. Layer iii: PMMA layer with the transition chamber. Layer iv: PSA, with a cut-out in the shape of the deflecting latex membrane. Layer v: The featureless, transparent, and elastic latex film. Layer vi is similar to the fourth layer—a PSA layer with a cut-out in the shape of the deflecting latex membrane. Layer vii: PMMA disk with the engraved air chamber.

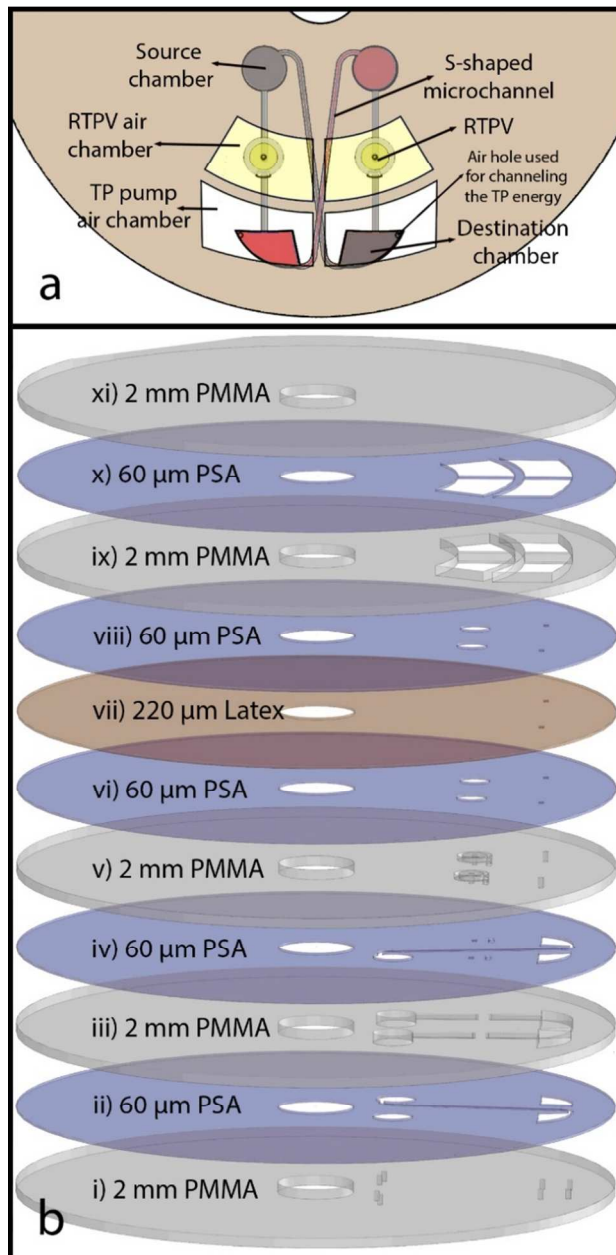


Figure 3. Microfluidic disk Design B. (a) This microfluidic disk is used for the continuous circulation and switching of two liquid samples. (b) Assembly of the eleven layer microfluidic disk consisting of five PMMA layers, five PSA layers, and a latex film. Layer i: PMMA disk with vent and loading holes. Layer ii: PSA layer with cut-outs in the shape of the loading and destination chambers and one of the two S-shaped microchannels connecting the destination chamber (right) to the loading chamber (left). Layer iii: PMMA disk with loading and destination chambers and engraved microchannels. Layer iv: PSA layer with the vertically reflected features of layer ii and additional cut-outs in the shape of the inlet and outlet. Layer v: PMMA disk with the transition chambers and two through-holes to connect the upper layer air chambers to the lower layer destination chambers. Layer vi: PSA with cut-outs matching the shapes of the elastic membranes and the through-holes. Layer vii: a featureless latex film. Layer viii: PSA with cut-outs and through-holes similar to the layer vi. Layer ix: PMMA disk with cut-outs in the shapes of the ventless air chambers used for RTPVs and TP pumps. Layer x: PSA with cut-outs in the shapes of the elastic membranes similar to layer ix and layer xi A featureless PMMA layer that seals the air chambers from the top side of the disk. It should be noted that the top three layers could be replaced by a thicker PMMA layer with engraved air chambers, but in that case, the engraved features could reduce the optical transparency of the disk.

platforms. Design A was first implemented to assess the RTPV behaviour from the closed to the open state as a function of the air chamber surface temperatures at various rotational frequencies (see Figure 2.a). The same design was also used to theoretically and experimentally analyse the cooling of a heated spinning disk. Design A is a seven-layer disk and is composed of a latex film, polymethyl-methacrylate (PMMA) disks, and pressure-sensitive adhesive (PSA) layers (see Figure 2.b). Design B (see Figure 3.a) is a microfluidic system specifically designed for continuous circulation and switching of two liquid samples. Design B was used to test the valve's reversibility, gas-impermeability, and ability to control the direction of the TP energy propagation in complex fluidic networks. The design is composed of two RTPVs, two sets of TP pumps, and two S-shaped microchannels cut out in two different PSA layers of the disk. The breakdown of the eleven-layer CD Design B is shown in Figure 3.b. The air chambers near the centre are used to generate TP energy for valving purposes and the other two are used for pumping liquids. Design C (see Figure 4.a) is a microfluidic cartridge created for the conversion of Dengue viral RNA to cDNA and the preparation of PCR reaction mixtures through the sequential aliquoting of the corresponding reagents into reaction chambers. Fluidic components and the

breakdown of the eleven-layer cartridge are demonstrated in Figure 4. The cartridge consisted of five PMMA layers, five PSA layers, and a latex film with a similar arrangement as Design B. The microfluidic platforms, are fabricated by the manual assembly of transparent PMMA layers (2 mm thick), PSA (~60 μm thick), and a latex film (~220 μm thick). The micro-features were machined into the PMMA disks using the Vision Engraving & Routing Systems computer numerical control (2525 CNC Router/Engraver, Vision, USA). The micro features in the PSA layers were cut-out using a PUMA II cutter plotter machine (GCC, Taiwan).

2.3. Experimental setup and procedure

A custom-made experimental setup used in this study consists of an automated CD spin stand and a semi-automated heating platform that controls the disk surface temperature. The spin monitoring system is comprised of a spinning motor, a laser RPM sensor, and a high-speed camera (Basler piA640-210gc, Germany), which were controlled by a custom-made LabVIEW program. The heating system is composed of a Bosch GHG 630 DCE modified industrial grade heat gun and an infrared thermometer (Smart Sensor AR550). The heat gun had a built-in digital temperature controller, which can produce air at any temperature between 50 and 500 $^{\circ}\text{C}$. The air heat gun had to be adjusted to significantly higher temperatures than the desired constant platform temperature. The details of the heating profile of a spinning disk with a similar thickness to that of Design A were reported previously.⁴⁴ The air heat gun temperature setting can be changed in steps of 10 $^{\circ}\text{C}$, and such a heating rig does not provide a precise control over temperature of the spinning disk. Hence, the valve's actuation temperature was evaluated during a ramped cool-down of the disc.

Although the air chamber adjacent to the latex membrane is ventless, a through hole was machined into the top PMMA layer and sealed just before the experimental procedure to prevent any pressure build up during the fabrication process. Then, 70 μl of coloured DI-water was dispensed into the source chamber. The experiment was initiated by spinning the disk and then heating the radial region of the valve while its surface temperature was continuously monitored. The rotational frequency was kept below 500 RPM (i.e., the average burst frequency of the valve at room temperature), and the surface temperature was heated until it reached 55 $^{\circ}\text{C}$ or 73 $^{\circ}\text{C}$ (for spin rates higher and lower than 2000 RPM, respectively) to make sure that the valves were closed by means of the deflection of the latex membrane. To characterize the conditions required to open the valve, the spinning speed was increased to a series of fixed rotational frequencies ranging from 700 RPM to 2500 RPM, all of which were higher than the burst frequency. When a new, higher spinning speed was reached, the heat source was turned off and the cooling process was initiated (see Figure 5.a). As soon as the pneumatic pressure in the valve dropped below the fixed centrifugally induced hydrostatic pressure, the valve was opened and liquid was transferred to the destination chamber (see Figure 5.b). During the cooling process, the critical temperatures corresponding to the opening of the valve were recorded. The entire liquid volume was gradually and smoothly drained from the source chamber, possibly due to the simultaneous reduction of the centrifugal pressure and the TP pressure in the valve (see Figure 5.c). The experiments were repeated five times, and the critical temperatures corresponding to the range of rotational frequencies were recorded.

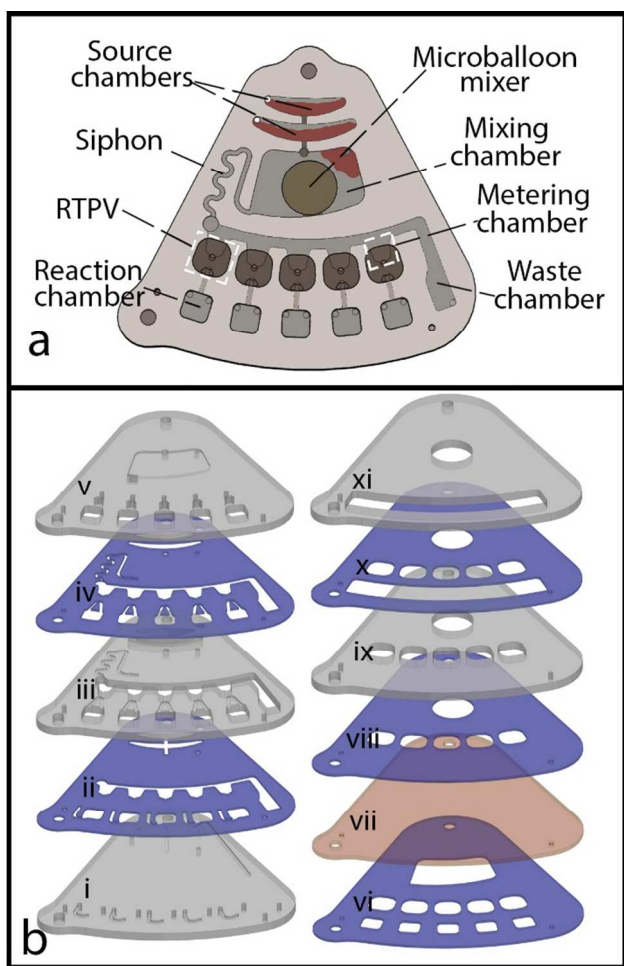


Figure 4. Microfluidic cartridge Design C. (a) Fluidic components of the cartridge used for preparation of PCR reaction mixture through sequential aliquoting. (b) Assembly of the eleven-layer platform consisting of five PMMA layers, five PSA layers, and a latex film.

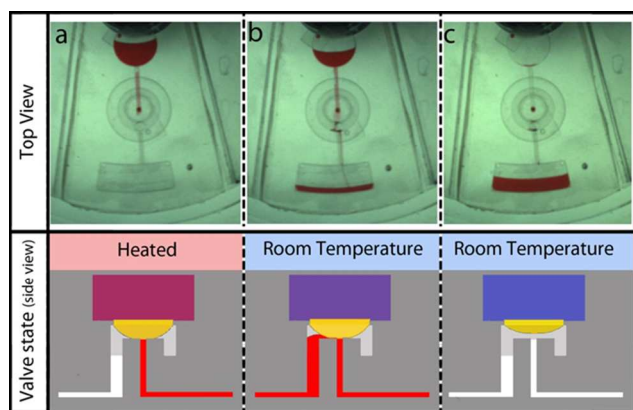


Figure 5. The RTPV mechanism as demonstrated on a microfluidic disk. (a) The heated valve closes, preventing fluid flow which can stand up to a certain centrifugal force. (b) Liquid flow across the valve once the centrifugal pressure overcomes the valve pressure. (c) Once the disk cools adequately, the entire liquid volume is drained from the source chamber.

Optimizing the spinning speed of the platform and the intensity of the heat source enabled the desired heating and cooling control of the disk, therefore allowing timing of the RTPVs' actuation. To further study and characterize cooling in the system, the times that it took for the surface temperature of the heated spinning disk to decrease from 40 °C to 28 °C were recorded.

3. Theoretical analysis

Characterization of the valve aids in its appropriate implementation in complex multi-step sequential assays. In this section, the RTPV actuation mechanism, which was implemented through heating and cooling on a centrifugal microfluidic platform, is theoretically analysed using the ideal gas law, the membrane deflection equation, and the equation for transient heat transfer of a freely rotating disk. The RTPV valving mechanism is characterized by calculating the valve's critical actuation temperatures and cooling time.

3.1. RTPV's actuation temperatures

When the ventless air chamber is heated, the pressure from the deflected membrane acting on the liquid inlet is equivalent to the difference between the induced TP pressure ΔP_{TP} and the pressure P_m required to deflect the membrane:

$$\Delta P_{RMV} = \Delta P_{TP} - P_m \quad (1)$$

According to the ideal gas law, ΔP_{TP} is given by:

$$\Delta P_{TP} = \frac{nRT}{V_{TP}} - \frac{nRT_0}{V_0} \quad (2)$$

where n is the number of moles, R is the ideal gas constant, T_0 and T are the temperatures at room temperature and when heated, respectively, and V_0 and V_{TP} are the volumes of the ventless air chamber at room temperature and when heated, respectively. For a known distance z between the membrane and the inlet, V_{TP} is given by:

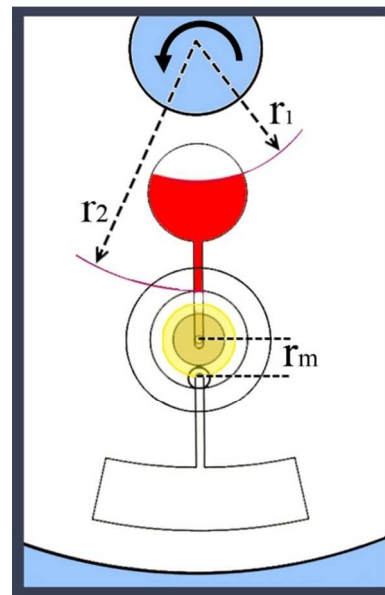


Figure 6. Showing the various parameters used in designing and controlling the RTPV, r_1 and r_2 are the radial distances of the liquid from the centre of the disk, and r_m is the membrane radius.

$$V_{TP} = V_0 + V_{mb} = V_0 + \frac{2}{3}\pi r_m^2 z \quad (3)$$

where r_m is radius of the membrane, and V_{mb} is the expanded air volume. For small value of z , where $V_0 \gg V_{mb}$, it is assumed that $V_{TP} \cong V_0$. The maximum possible value of z in the current study is $\sim 60 \mu\text{m}$, and based on this, the difference between V_{TP} and V_0 is less than 0.01%. Hence, from Equation 3 TP pressure is given as:

$$\Delta P_{TP} = \frac{nR\Delta T}{V_{TP}} \quad (4)$$

The pressure required to deflect the membrane to a height z is defined by the following equation (i.e., membrane bulge equation) that is a function of the membrane's Young's modulus of elasticity E , the radius of the membrane r_m , Poisson's ratio ν , the thickness of the elastic membrane j , initial stress σ_0 , and constants C_a and C_b (which may vary depending on the geometry of the membrane):^{32, 45, 46}

$$P_m = C_a \frac{Ejz^3}{r_m^4(1-\nu)} + C_b \frac{\sigma_0 jz}{r_m^2} \quad (5)$$

Substituting Equations 4 and 5 into Equation 2, the valve pressure is then given by:

$$\Delta P_{RMV} = \frac{nR\Delta T}{V_{TP}} - \left(C_a \frac{Ejz^3}{r_m^4(1-\nu)} + C_b \frac{\sigma_0 jz}{r_m^2} \right) \quad (6)$$

Except for the temperature and the height of the bulged membrane, all the parameters in the equation are constant. Assuming the valve deflection at the instant the valve actuates is insignificant ($\Delta z \approx 0$), the valve pressure varies only by the change of temperature ΔT . Therefore, the minimum increment of temperature that is required to prevent flow at a fixed

rotational frequency can be predicted by equalling the valve pressure and the induced centrifugal pressure:

$$\Delta P_{\omega} = \rho \omega^2 \Delta r \bar{r} \quad (7)$$

where ρ is the density of liquid, $\bar{r} = (r_2 + r_1)/2$ is the average distance of the liquid from the centre of the disk, $\Delta r = (r_2 - r_1)$ is the radial length of the liquid inside the microfluidic system, and ω is the rotational frequency of the disk (see Figure 6). By balancing the valve and centrifugal pressures, measured from Equation 6 and Equation 7, the valving condition to prevent flow can thus be characterized as:

$$\frac{nR\Delta T}{V_{TP}} - \left(C_a \frac{Ejz^3}{r_m^4(1-\nu)} + C_b \frac{\sigma_0 jz}{r_m^2} \right) > \rho \omega^2 \Delta r \bar{r} \quad (8)$$

To simplify Equation 8, we define two constant values, $K_1 = \rho \Delta r \bar{r} / 2$ and $K_2 = (nR/V_{TP})$. The critical temperature required to prevent flow for a known rotational frequency and room temperature is defined as follows:

$$T > \frac{K_1 \omega^2 + K_2 T_0 + P_m}{K_2} \quad (9)$$

We have compared the experimentally measured and theoretically obtained actuation temperatures of a RTPV at various fixed rotational frequencies to test the accuracy of Equation 9 (see results and discussion section).

3.2. RTPV's cooling time

The calculation of the passive cooling time of a heated spinning disk is based on several factors, mainly the room temperature value and the air flow regime existing around the disk at a certain spinning speed. The existing flow regime in the system depends on the range of rotational frequency and can be determined by the value of the Reynolds number given as:

$$Re = \frac{\omega d}{\vartheta} \quad (10)$$

where d and ϑ are the disk diameter and kinematic viscosity of air, respectively. In accordance with Equation 10, the dominant flow regime under the current testing conditions is laminar, and the heat transfer for the laminar regime around the disk is based on the "one-dimensional conduction of heat in a semi-infinite slab with a convective boundary condition".⁴⁷⁻⁴⁹

$$\theta = \frac{T - T_{\infty}}{T_C - T_{\infty}} = e^{\gamma^2} \cdot \text{erfc}(\gamma) \quad (11)$$

where, T_C is the disk surface temperature increased above the critical value T . γ is defined as:

$$\gamma = \frac{K_T k}{k_d} \sqrt{\frac{a_d \omega t}{Pr a}} \quad (12)$$

where, K_T is a constant,⁴⁷ Pr is the Prandtl number of air, a and k are thermal diffusivity and thermal conductivity of air, respectively, and a_d and k_d are thermal diffusivity and thermal conductivity of the disk (PMMA), respectively. For convenience, we have defined:

Table 1. Values of the significant parameters used in the theoretical analysis.

Parameters	Value	Parameters	Value
N	1.7488×10^{-5}	r_1	15 mm
R	8.31 J(Mol.K)	r_2	32 mm
T_0	26°C	Pr	0.71
V_0	$4.287 \times 10^{-7} \text{ m}^3$	a	$2.43 \times 10^{-5} \text{ m}^2/\text{s}$
r_m	3.5 mm	a_d	$1.2 \times 10^{-7} \text{ m}^2/\text{s}$
E	1.2 MPa	k	$27 \times 10^{-3} \text{ W/(m.k)}$
σ_0	0.059 MPa	k_d	0.17 W/(m.k)
J	220 μm	A	0.003
N	0.48	B	0.0446
C_a	8/3	C	0.2858
C_b	4	D	0.2678

$$\zeta = \frac{K_T k}{k_d} \sqrt{\frac{a_d \omega}{Pr a}} \quad (13)$$

For the cooling of the rotating disk used in the current, we have experimentally defined the expression value of K_T :

$$K_T = A\Delta T^3 - B\Delta T^2 + C\Delta T - D \quad (14)$$

where, A , B , C , and D are experimentally derived constants. The following equation results upon substituting Equations 12, 13, and 14 into Equation 11:

$$1 = \frac{e^{\gamma^2} \text{erfc}(\zeta t^{1/2})}{\theta} \quad (15)$$

For fixed rotational frequencies, Equation 15 can be numerically solved to obtain the required cooling time for changing the surface temperature from T_C to T .

A comparison between the experimentally recorded cooling times and time periods measured by Equation 15 is presented in Figure 7.c (see Section 4). The values of the different parameters used in the theoretical analysis of the RTPV mechanism are listed in Table 1.

4. Results and discussion

Several valving designs were tested to identify characteristics of the RTPV that allow for the most efficient use of the TP energy and to maximize the accessible range of rotational frequencies. We initially aligned the latex membrane parallel to a microchannel with a small opening that accommodated the deflection of the membrane. However, such an arrangement did not result in robust sealing due to the gaps remaining between the corners of the valve seat and the deflected membrane. This problem led us to use a transition chamber with a vertical microchannel (inlet) perpendicular to the latex membrane. The ultra-short distance between the membrane and the top of the inlet significantly limited the deflection of the latex membrane, allowing for the efficient use of TP energy for a robust sealing of the inlet. Efficient use of TP energy, which enables the valve to operate by small changes

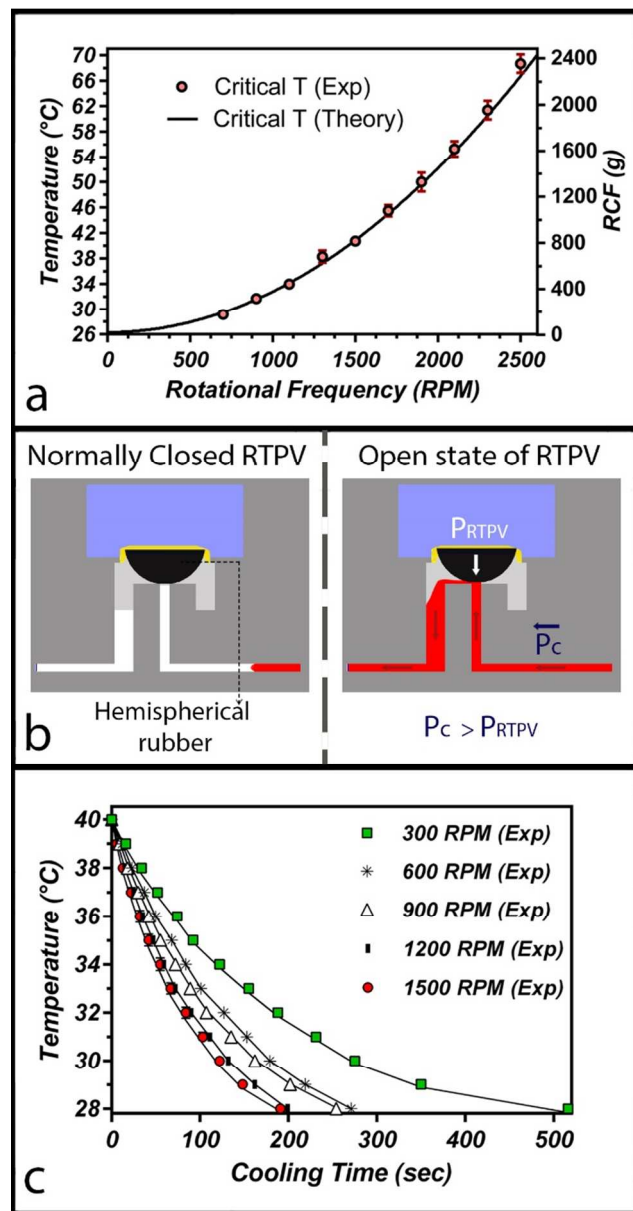


Figure 7. (a) The temperatures in which the centrifugal pressure is equal to RTPV pressure. Experimentally measured critical temperatures corresponding to transition of RTPV from the closed to the open states are shown by markers. It should be noted that the experimental burst frequency of the valve at room temperature is approximately 500 RPM. Maximum relative centrifugal field (RCF) is provided in the graph to facilitate incorporation of the design into future microfluidic platforms. (b) Schematics of closed and open state of the normally-closed RTPV with the embedded hemispherical rubber seal. (c) The cooling process of the heated disk spinning at various rotational frequencies. The markers indicate the experimental data while the lines are values calculated from Equation 15.

in temperature, is of great importance in clinical assays, where reactions may occur near body temperature. For instance, the optimal range of operating temperature for nucleic acid sequence-based amplification (NASBA) and recombinase polymerase amplification (RPA) are within the range of 37–42 °C.^{50, 51} In Figure 7.a, we compare the experimentally measured critical temperatures of an RTPV with the theoretical ones

obtained from Equation 9. Good agreement between the experimental data and the predicted values is observed from room temperature to 70 °C and at spinning speeds from 700 RPM to 2500 RPM. Hence, Equation 9 provides an accurate prediction of the valve's actuation temperatures at various spinning speeds. To retain liquids at higher spinning speeds, the valve requires a higher temperature that is beyond the operational temperature of the disk materials used in this study. To circumvent these challenges, an extra hemispherical rubber seal can be embedded between the latex layer and the transition chamber, dramatically increasing the range of operational rotational frequency while also making the valve a normally-closed valve (see Figure 7.b). Preliminary experiments show that by adding a 2 mm hemispherical rubber seal to the same radial location in the system and varying the membrane diameter (from 6 mm to 16 mm in radius), centrifugally generated hydrostatic pressures at decreasing spinning speeds of 6000 RPM down to 1300 RPM are required to open the normally-closed valve. As the membrane diameter decreases, the initial valve pressure is enhanced, and therefore, a higher spinning speed is required to actuate the RTPV (e.g., a membrane of 6 mm diameter requires 6000 RPM to open). In the designs introduced in the current study, the air chambers are located above the latex membranes; however, air chambers can be positioned anywhere in the microfluidic disk and linked with the membrane through microchannels. This facilitates the control of TP energy input and sequential valving in multi-stage operations particularly when a set of RTPVs are aligned on the same radius of the microfluidic disk.

To fully automate a sequential microfluidic procedure with RTPVs, we need to control the valves' actuation temperatures and predict their response times. Figure 7.c shows the comparison between the cooling times recorded from experiments and those calculated at different rotational frequencies using Equation 15, an empirical equation. This figure shows an excellent agreement between the experimental data and the values predicted by Equation 15. Design B was 2.12 mm thicker than Design A and required slightly longer cooling periods. This is expected as the thermal resistance of the thicker platform is higher. In cooling experiments conducted with Design B at spin rates of 600 rpm and 1200 rpm, 10 seconds and 23 seconds longer times were required to reduce the temperature from 40 °C to 28 °C, respectively. In general, over a wider temperature range and for different disk materials and thicknesses, the parameter K_T in Equation 14 should be experimentally redefined. The difference between the required heating times of the two platforms, on the other hand, was negligible. This is also expected because the heating periods in these experiments, and in experiments reported in the previous study,⁴⁴ are much shorter than the cooling periods.

The obvious limitations of the heating setup (e.g., slow operation, high power consumption, etc.) limit its usage as a thermal-cycler in assays (e.g., PCR amplification) that require rapid and precise changes of temperature. However, the aim of this study was to develop a reversible valve facilitating fluidic procedures on a microfluidic disk, which automatically closes to prevent evaporation of reagents at elevated temperatures. The RTPV is expected to operate smoothly with both contact, and non-contact heating systems such as a laser-based heating setup used for isothermal DNA amplification assays,⁵¹ or the air-mediated heating-cooling setup used in the Rotor-Gene 2000 for real time PCR amplification.^{18, 52, 53} Nevertheless, the heating setup was successfully used in continuous liquid circulation/switching, and sequential aliquoting applications,

which are described in the next section. Sequential aliquoting allowed for the preparation of PCR reaction mixtures required for the detection of Dengue virus.

5. RTPV Applications

5.1. Continuous liquid circulation/switching

Liquid circulation in microfluidic devices is used for applications such as serial dilution,⁵⁴ DNA hybridization,^{55, 56} and micromixing.⁵⁷ In addition, liquid circulation is widely used to control residence time distribution in chemical and biological reactors and to achieve and preserve desired flow patterns.⁵⁸ In centrifugal microfluidics, continuous liquid circulation has great potential in enhancing the rate of analyte capture, leading to faster detection in bioassays.⁵⁹

With Design B, we demonstrated continuous liquid circulation on a spinning disk by means of a pair of RTPVs and a pair of TP pumps. The reversibility and the gas-impermeability of the technology facilitate precise control of TP energy input and liquid flow. The vapour tight seals of RTPV enables control source chambers. A step-by-step demonstration of the liquid circulation experiment is shown in Figure 8 (Video 1 showing the circulation of liquids is available in the supplementary section). Two liquid samples, blue and red, were introduced into the source chambers (see Figure 8.a). The disk was then spun at 900 RPM, transferring the liquids

into the destination chambers (see Figure 8.b). When the liquids were completely drained from the source chambers into the destination chambers, the rotational frequency was reduced to 300 RPM (see Figure 8.c). Due to the ultra-short distance between the liquid inlet and the membranes in the RTPVs, a small temperature increment caused the membrane to seal the inlets before the TP pumps were able to transfer the liquids towards the source chambers. A further increase in temperature actuated the TP pumps to propel the liquids towards the disk centre along the S-shaped channels (see Figure 8.d). The disk was continuously heated until both liquids were transferred to the opposite source chambers (see Figure 8.e). To test the reversibility of the valving system, the RTPVs were then reopened by cooling them by fast spinning (see Figure 8.f, g). In Figures 8.h to 8.i, the liquids were further circulated until they were transferred back to their initial source chambers once more.

5.2. Sequential aliquoting

Design C was developed for sequential aliquoting to demonstrate applicability of microballoon valve/pumping for automation fluidic procedures commonly required for multiplexing of heat-based assays. Aliquoting a large reagent volume into several reaction chambers by means of an array of metering fingers (chambers) and valves is the key fluidic step in multiplexing any analytical assay on a microfluidic disk. Except the CP valve, which is regenerated after each actuation,¹⁸ no other introduced reversible or sacrificial valves were suitable for sequential aliquoting of reagents. However, the CP valve is not robust in designs with large reaction chambers, and it is usually used on platforms made from highly hydrophobic foil material.^{18,60} On the other hand, aliquoting is popular for multiplexing of the heat-based assays, in which the integration of the gas-impermeable valves is considered a great advantage to prevent the evaporation of miniaturized reagents and the risk of cross-contamination.^{24, 26, 50, 61} To demonstrate the ability of the new valving system to overcome those challenges, an array of RTPVs is embedded in microfluidic Design C, which is created to automate the fluidic procedures commonly required for the multiplexing of heat-based assays. As a pilot study, Design C was used for the conversion of Dengue viral RNA to cDNA, and for the preparation of PCR reaction mixtures. The reversibility of RTPVs allowed for sequential aliquoting of Dengue virus RNA and PCR master mix, to multiple separated PCR reaction mixtures. Moreover, the ability of the valve to automatically close at elevated temperature prevented the evaporation of reagents during thermocycling period.

A step-by-step visualization of the assay integrated in the cartridge is demonstrated in Figure 9.A. Briefly, four of the reaction chambers were loaded with 0.2 μg (2 μl) of Dengue virus RNA and 2 μl DI-water was injected into the fifth reaction chamber, which was used as the negative control. Dengue virus RNA was isolated from Dengue-infected cells using a commercially available kit (Promega, USA). Afterwards, 110 μl of the RT master mix (Applied Biosystem, USA) was charged into the cartridge, and all injection holes were sealed. The spin rate was immediately increased to 1800 rpm to make sure the microballoon sufficiently expanded with the reagent entering the mixing chamber and prevent the overfilling of the mixing chamber. The platform was heated to change the RTPVs from the open to the closed state. After a minute, the spin rate was reduced to 300 rpm to contract the microballoon. Releasing elastic energy of the expanded microballoon pumped

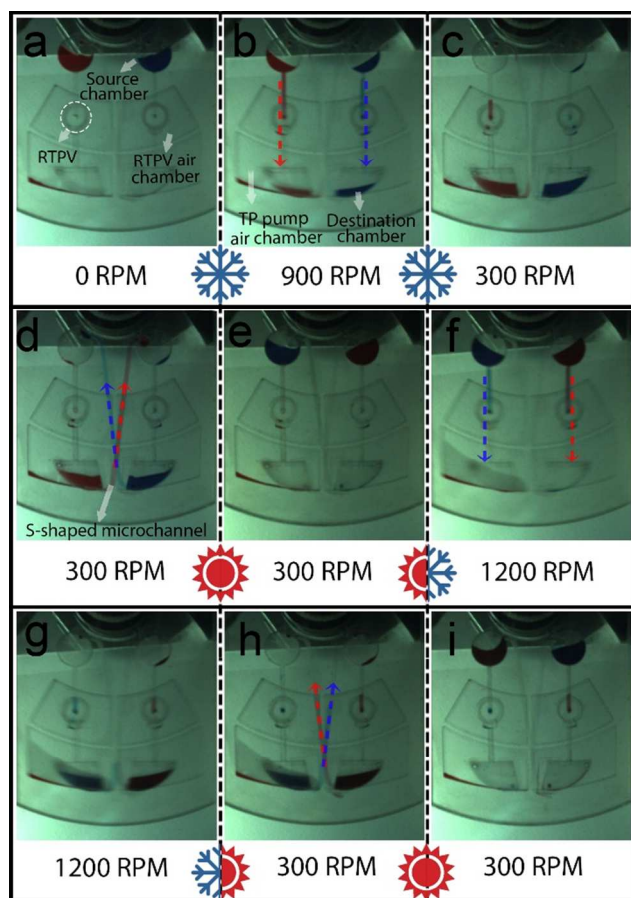


Figure 8. Sequential events in the microfluidic disk designed for continuous liquid circulation. The fluidic system consists of two RTPVs and two TP pumps, allowing for real-time flow control.

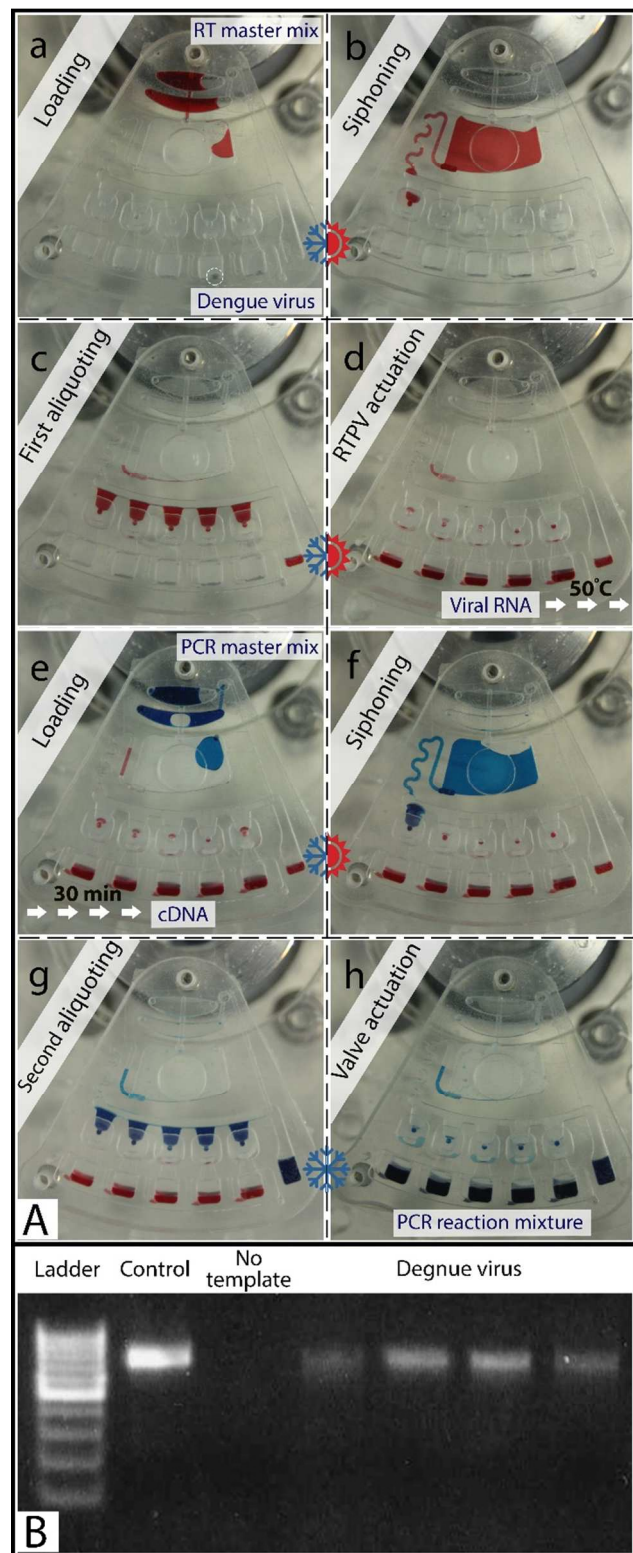


Figure 9. The microfluidic cartridge designed for automation of thermally controlled assays. (A) Sequential aliquoting for preparation of PCR reaction mixture. (B) The agarose gel electrophoresis for analysing PCR reactions, and risk of cross contamination during thermocycling period.

the reagent against the direction of centrifugal force, increased the liquid level inside the mixing chamber and primed the siphon valve (see Figure 9.b). Aliquoting the master mix into the metering chambers of 20 μ l occurred by increasing the spin rate to 1000 rpm (see Figure 9.c). The heat source was powered off for 1 minute, and spin rate was increased to 3000 rpm to immediately open (actuate) the RTPVs and transfer the aliquoted reagents into their corresponding reaction chambers (see Figure 9.d). The cartridge was then spun at 300 rpm and kept at 50 $^{\circ}$ C for 30 minutes to convert Dengue viral RNA to cDNA. In the next reagent-refilling step, the components required for the preparation of 120 μ l of fresh PCR master mix were distributed into the loading and mixing chambers (see Figure 9.e). The PCR master mix contained 60 μ l of 2X PCR mixture (Promega, USA), 6 μ l Dengue Forward primer, 6 μ l Dengue reverse primer, and 48 μ l dH₂O. The PCR master mix was prepared through microballoon mixing by altering the spin rate of the disk between 2600 and 2000 rpm for 30 seconds. In Figures 9.f to 9.h, the mixed reagent was aliquoted into the reaction chambers by the similar fluidic procedure demonstrated in figure 9.b to figure 9.d. The heating setup and platform material could not support the PCR thermal-cycling profile. Therefore, the multiplexed PCR reaction mixtures were transferred into tubes, and PCR reaction was performed in a conventional thermal-cycler to evaluate the quality of the assay. The thermal-cycling profile of the PCR reaction included 2 minutes denaturation at 95 $^{\circ}$ C, 40 cycles of 95 $^{\circ}$ C (30 seconds), 55 $^{\circ}$ C (30 seconds), and 72 $^{\circ}$ C (30 seconds), and 10 minutes extension at 72 $^{\circ}$ C. PCR products then were visualized by agarose gel electrophoresis (Figure 9.B). The agarose gel electrophoresis analysis indicated that reaction in the 4 wells was successful and there was no cross-contamination during the thermocycling period, since there is no band in the negative control. In addition, the PCR product of the positive control (the conventional method of reverse transcription and PCR) showed a similar result compared to our methods as evidenced by the gel image.

At elevated temperatures, built-up TP pressure in the air chambers of RTPVs suppresses the rising pressure inside the heated reaction chambers, preventing the evaporation of reagents and cross-contamination. Perhaps no evaporation of reagents was observed or even expected at 50 $^{\circ}$ for 30 minutes. Therefore, the efficiency of the RTPV to prevent evaporation of reagent at more elevated temperatures was demonstrated by using the thermocycling profile of a LAMP assay, i.e., 1 hour of 65 $^{\circ}$ C followed by 2 minutes at 80 $^{\circ}$ C (Video 2 showing the evaporation of heated liquids inside chambers with and without RTPVs is available in the supplementary section). In general, the reversibility of RTPVs and their sensitivity to changes in temperature creates a unique valving system to automate fluidic procedures required for multiplexing of temperature-controlled assays.

6. Conclusions

We have developed the RTPV, a novel valving technique on centrifugal microfluidic platforms based on the thermal expansion of trapped air and the deflection of an embedded elastic membrane. Unlike conventional, single-use active valves that utilize thermal energy to remove barriers to permit liquid flow, the RTPV is a reversible mechanism that manipulates thermal energy to reversibly block or open microchannels. The air expansion in the heated air chamber deflects the latex membrane, sealing the inlet and preventing fluid flow. The

valving mechanism was modelled and experimentally investigated over a range of rotational speeds from 700 to 2500 RPM, and temperatures from 26 to ~70 °C. The ability of the valve to prevent flow during heating makes RTPVs suitable for use in heat-based applications such as PCR, LAMP and NASBA. Particularly, the small magnitude of temperature changes involved in the closed state of the RTPV accommodates valving needs in diagnostic assays where biological reactions occur near body temperature. By defining an empirical equation that predicts the cooling process of a heated disk during spinning, we have enabled the development of time-programmable RTPVs. The usability of the valving mechanism in various applications such as micromixing and DNA hybridization are demonstrated through continuous liquid circulation and sequential aliquoting of reagents, respectively. Overall, RTPV offers unique advantages for controlling fluid flow that facilitate the integration of intricate biochemical assays on microfluidic disk.

Acknowledgements

This research was supported by University of Malaya (UM) High Impact Research Grant UM-MOHE UM.C/625/1/HIR/MOHE/05 from the Ministry of Higher Education Malaysia (MOHE), and University of Malaya Research Grant (UMRG RP009A-13AET). Fatimah Ibrahim would like to acknowledge Yayasan Sultan Iskandar Johor Foundation for funding the Special Equipment Grant. Marc Madou acknowledges support of the National Institute of Health (NIH) Grant 1 R01 AI089541-01. M. Mahdi Aeinehvand would like to thank Ling Kong for her invaluable assisting with preparation of the manuscript.

Notes and references

^a Centre for innovation in medical engineering(CIME), Department of Biomedical Engineering, Faculty of Engineering, University of Malaya, 50603 Kuala Lumpur, Malaysia. Tel: 603-7967-6818; E-mail: fatimah@um.edu.my

^b Department of Electrical Engineering, Faculty of Engineering, University of Malaya, 50603 Kuala Lumpur, Malaysia.

^c Department of Molecular Medicine, Faculty of Medicine University of Malaya, 50603 Kuala Lumpur, Malaysia.

^d Department of Biomedical Engineering, University of California, Irvine, Irvine, 92697, United States.

^e Department of Mechanical and Aerospace Engineering, University of California, Irvine, Irvine, 92697, United States.

1. G. M. Whitesides, *Nature*, 2006, **442**, 368-373.
2. K. Abi-Samra, T.-H. Kim, D.-K. Park, N. Kim, J. Kim, H. Kim, Y.-K. Cho and M. Madou, *Lab on a Chip*, 2013, **13**, 3253-3260.
3. J.-M. Park, M. S. Kim, H.-S. Moon, C. E. Yoo, D. Park, Y. J. Kim, K.-Y. Han, J.-Y. Lee, J. H. Oh and S. S. Kim, *Analytical chemistry*, 2014, **86**, 3735-3742.
4. E. Roy, G. Stewart, M. Mounier, L. Malic, R. Peytavi, L. Clime, M. Madou, M. Bossinot, M. G. Bergeron and T. Veres, *Lab on a Chip*, 2015, **15**, 406-416.
5. T. van Oordt, G. B. Stevens, S. K. Vashist, R. Zengerle and F. von Stetten, *RSC Advances*, 2013, **3**, 22046-22052.
6. R. Burger and J. Duce, 2012.
7. C. E. Nwankire, M. Czugala, R. Burger, K. J. Fraser, T. Glennon, B. E. Onwuliri, I. E. Nduaguibe, D. Diamond and J. Duce, *Biosensors and Bioelectronics*, 2014, **56**, 352-358.
8. C. E. Nwankire, D.-S. S. Chan, J. Gaughran, R. Burger, R. Gorkin and J. Duce, *Sensors*, 2013, **13**, 11336-11349.
9. R. Gorkin III, C. E. Nwankire, J. Gaughran, X. Zhang, G. G. Donohoe, M. Rook, R. O'Kennedy and J. Duce, *Lab on a Chip*, 2012, **12**, 2894-2902.
10. R. Gorkin, J. Park, J. Siegrist, M. Amasia, B. S. Lee, J.-M. Park, J. Kim, H. Kim, M. Madou and Y.-K. Cho, *Lab on a Chip*, 2010, **10**, 1758-1773.
11. O. Strohmeier, M. Keller, F. Schwemmer, S. Zehnle, D. Mark, F. von Stetten, R. Zengerle and N. Paust, *Chemical Society Reviews*, 2015.
12. A. Kazemzadeh, P. Ganesan, F. Ibrahim, M. M. Aeinehvand, L. Kulinsky and M. J. Madou, *Sensors and Actuators B: Chemical*, 2014, **204**, 149-158.
13. N. Godino, R. Gorkin III, A. V. Linares, R. Burger and J. Duce, *Lab on a Chip*, 2013, **13**, 685-694.
14. R. Burger, M. Kitsara, J. Gaughran, C. Nwankire and J. Duce, 2014.
15. M. Kitsara, C. E. Nwankire, L. Walsh, G. Hughes, M. Somers, D. Kurzbuch, X. Zhang, G. G. Donohoe, R. O'Kennedy and J. Duce, *Microfluidics and Nanofluidics*, 2014, **16**, 691-699.
16. C. E. Nwankire, G. G. Donohoe, X. Zhang, J. Siegrist, M. Somers, D. Kurzbuch, R. Monaghan, M. Kitsara, R. Burger and S. Hearty, *Analytica chimica acta*, 2013, **781**, 54-62.
17. A. Kazemzadeh, P. Ganesan, F. Ibrahim, L. Kulinsky and M. J. Madou, *RSC Advances*, 2014.
18. O. Strohmeier, N. Marquart, D. Mark, G. Roth, R. Zengerle and F. von Stetten, *Analytical Methods*, 2014, **6**, 2038-2046.
19. C. E. Nwankire, M. Czugala, R. Burger, K. J. Fraser, T. M. O'Connell, T. Glennon, B. E. Onwuliri, I. E. Nduaguibe, D. Diamond and J. Duce, *Biosensors and Bioelectronics*, 2014.
20. D. J. Kinahan, S. M. Kearney, N. Dimov, M. T. Glynn and J. Duce, *Lab on a Chip*, 2014, **14**, 2249-2258.
21. N. Dimov, E. Clancy, J. Gaughran, D. Boyle, D. Mc Auley, M. T. Glynn, R. M. Dwyer, H. Coughlan, T. Barry and L. M. Barrett, *Microfluidics and Nanofluidics*, 2014, **18**, 859-871.
22. H. Hwang, H.-H. Kim and Y.-K. Cho, *Lab on a Chip*, 2011, **11**, 1434-1436.
23. T.-H. Kim, K. Abi-Samra, V. Sunkara, D.-K. Park, M. Amasia, N. Kim, J. Kim, H. Kim, M. Madou and Y.-K. Cho, *Lab on a Chip*, 2013, **13**, 3747-3754.
24. M. Amasia, M. Cozzens and M. J. Madou, *Sensors and Actuators B: Chemical*, 2012, **161**, 1191-1197.
25. W. Al-Faqheri, F. Ibrahim, T. H. G. Thio, J. Moebius, K. Joseph, H. Arof and M. Madou, *PLoS one*, 2013, **8**, e58523.
26. L. X. Kong, K. Parate, K. Abi-Samra and M. Madou, *Microfluidics and Nanofluidics*, 2014, 1-7.
27. W. Al-Faqheri, F. Ibrahim, T. H. G. Thio, M. M. Aeinehvand, H. Arof and M. Madou, *Sensors and Actuators A: Physical*, 2014.
28. L. Swayne, A. Kazarine, E. J. Templeton and E. D. Salin, *Talanta*, 2015, **134**, 443-447.
29. J.-M. Park, Y.-K. Cho, B.-S. Lee, J.-G. Lee and C. Ko, *Lab on a Chip*, 2007, **7**, 557-564.
30. J. L. Garcia-Cordero, D. Kurzbuch, F. Benito-Lopez, D. Diamond, L. P. Lee and A. J. Ricco, *Lab on a Chip*, 2010, **10**, 2680-2687.
31. Z. Cai, J. Xiang, B. Zhang and W. Wang, *Sensors and Actuators B: Chemical*, 2015, **206**, 22-29.
32. M. M. Aeinehvand, F. Ibrahim, W. Al-Faqheri, T. H. G. Thio, A. Kazemzadeh and M. Madou, *Lab on a Chip*, 2014, **14**, 988-997.
33. M. M. Aeinehvand, F. Ibrahim, S. W. Harun, I. Djordjevic, S. Hosseini, H. A. Rothan, R. Yusof and M. J. Madou, *Biosensors and Bioelectronics*, 2014.
34. A. K. Au, H. Lai, B. R. Utela and A. Folch, *Micromachines*, 2011, **2**, 179-220.
35. K. W. Oh and C. H. Ahn, *Journal of micromechanics and microengineering*, 2006, **16**, R13.
36. N. Abd Hamid, J. Yunas, B. Yeop Majlis, A. A. Hamzah, B. Bais and J. Atkinson, *Microelectronics International*, 2015, **32**.
37. M. J. Zdeblick, R. Anderson, J. Jankowski, B. Kline-Schoder, L. Christel, R. Miles and W. Weber, 1994.
38. E. T. Lagally, P. C. Simpson and R. A. Mathies, *Sensors and Actuators B: Chemical*, 2000, **63**, 138-146.

39. M. A. Unger, H.-P. Chou, T. Thorsen, A. Scherer and S. R. Quake, *Science*, 2000, **288**, 113-116.
40. V. Studer, G. Hang, A. Pandolfi, M. Ortiz, W. F. Anderson and S. R. Quake, *Journal of Applied Physics*, 2004, **95**, 393-398.
41. E. Lagally, I. Medintz and R. Mathies, *Analytical chemistry*, 2001, **73**, 565-570.
42. C. Zhang, D. Xing and Y. Li, *Biotechnology advances*, 2007, **25**, 483-514.
43. E. T. Lagally, C. A. Emrich and R. A. Mathies, *Lab on a Chip*, 2001, **1**, 102-107.
44. T. H. G. Thio, F. Ibrahim, W. Al-Faqheri, J. Moebius, N. S. Khalid, N. Soin, M. K. B. A. Kahar and M. Madou, *Lab on a Chip*, 2013, **13**, 3199-3209.
45. R. J. Hohlfelder, *Bulge and blister testing of thin films and their interfaces*, 1999.
46. M. J. Madou, *Fundamentals of microfabrication: the science of miniaturization*, CRC press, 2002.
47. I. V. Shevchuk, *Convective heat and mass transfer in rotating disk systems*, Springer, 2009.
48. T. Indinger and I. V. Shevchuk, *International Journal of Heat and Mass Transfer*, 2004, **47**, 3577-3581.
49. I. V. Shevchuk, *International Journal of Heat and Mass Transfer*, 2006, **49**, 3530-3537.
50. S. Lutz, P. Weber, M. Focke, B. Faltin, J. Hoffmann, C. Müller, D. Mark, G. Roth, P. Munday and N. Armes, *Lab on a Chip*, 2010, **10**, 887-893.
51. T.-H. Kim, J. Park, C.-J. Kim and Y.-K. Cho, *Analytical chemistry*, 2014, **86**, 3841-3848.
52. O. Strohmeier, S. Laßmann, B. Riedel, D. Mark, G. Roth, M. Werner, R. Zengerle and F. von Stetten, *Microchimica Acta*, 2013, 1-8.
53. M. Focke, F. Stumpf, B. Faltin, P. Reith, D. Bamarni, S. Wadle, C. Müller, H. Reinecke, J. Schrenzel and P. Francois, *Lab on a Chip*, 2010, **10**, 2519-2526.
54. S. Ahrar, M. Hwang, P. N. Duncan and E. E. Hui, *Analyst*, 2014, **139**, 187-190.
55. K. Rodaree, T. Matusos, S. Chaotheing, T. Pogfay, N. Suwanakitti, C. Wongsombat, K. Jaruwongrungee, A. Wisitsoraat, S. Kamchonwongpaisan and T. Lomas, *Lab on a Chip*, 2011, **11**, 1059-1064.
56. H. H. Lee, J. Smoot, Z. McMurray, D. A. Stahl and P. Yager, *Lab on a Chip*, 2006, **6**, 1163-1170.
57. P. K. Yuen, G. Li, Y. Bao and U. R. Müller, *Lab on a Chip*, 2003, **3**, 46-50.
58. L. Yerushalmi, M. Alimahmoodi, F. Behzadian and C. N. Mulligan, *Bioprocess and biosystems engineering*, 2013, **36**, 1339-1352.
59. J. L. Garcia-Cordero, L. Basabe-Desmonts, J. Ducrée and A. J. Ricco, *Microfluidics and nanofluidics*, 2010, **9**, 695-703.
60. F. Shen, E. K. Davydova, W. Du, J. E. Kreutz, O. Piepenburg and R. F. Ismagilov, *Analytical chemistry*, 2011, **83**, 3533-3540.
61. J. H. Jung, B. H. Park, S. J. Oh, G. Choi and T. S. Seo, *Biosensors and Bioelectronics*, 2015, **68**, 218-224.